Available online at www.sciencedirect.com
ScienceDirect
Journal of Sound and Vibration 299 (2007) 409–417
JOURNAL OF SOUND AND VIBRATION
www.elsevier.com/locate/jsvi

Short Communication

Error sensor location optimization for active soft edge noise barrier

Feng Niu[a,b,*], Haishan Zou[a], Xiaojun Qiu[a], Ming Wu[a]

[a]*Key Laboratory of Modern Acoustics and Institute of Acoustics, Nanjing University, Nanjing 210093, People's Republic of China*
[b]*Acoustics Laboratory, National Institute of Metrology, Beijing 100013, People's Republic of China*

Received 24 May 2006; received in revised form 3 August 2006; accepted 3 August 2006
Available online 25 September 2006

Abstract

Active control is used to improve the performance of noise barrier at low-frequency range and the excess insertion loss due to the active control system is influenced by the positions of the error sensors. The positional optimization for the error sensors in an active soft edge noise barrier was investigated. Both numerical simulations and experiments show that there is an optimum in the distance between the secondary sources and the error sensors, and that the error sensors should be placed above the secondary sources.

1. Introduction

The diffracted sound in the ''dark area'' of a noise barrier has been studied since the early days of 20th century, which the directed sound cannot reach. Li and Wong [1] summarized the calculating methods about the diffracted acoustic field after Sommerfled formulated the mathematically rigorous solution of a half-plane diffraction problem, and indicated that the methods could be implemented with two analytical solutions and two approximate solutions. The MacDonald solution is going to be used in this communication for calculating the insertion loss in actual designing the noise barrier.

To increase the noise control effect of the noise barrier, the active control system is used to decrease the low-frequency noise in the ''dark area''. When the active systems minimize the sound pressures along the barrier, the acoustic soft edge is formed, so this kind of active barrier is called active soft edge noise barrier. Omoto and Fujiwara [2] applied the active control system on the semi-infinite noise barrier to decrease the low-frequency noise, and validated availability of the active control system for the barrier through numerical simulations and experiments, then also Omoto et al. [3] investigated the influence of the ground reflection to the active control system through the experimental method, and obtained that the active system works normally with about 6 dB excess attenuation over the barrier's insertion loss at the receiver at a distance of 50 m. Studies on increasing the noise reduction effect of the barrier with the active control system when the

*Corresponding author. Tel.: +86 25 8359 4505; fax: +86 25 8359 2919.
E-mail address: niufeng@nju.org.cn (F. Niu).

0022-460X/$ - see front matter © 2006 Elsevier Ltd. All rights reserved.
doi:10.1016/j.jsv.2006.08.005

ground reflection exists is extended by Guo and Pan [4]. The influence of the geometry shape of the secondary sources was researched by Shao et al. [5], and based on Shao's results, Yang and Gan [6] discussed how to choose the cost function when the secondary sources are arranged the arc-type. Recently, Ohnishi et al. [7] applied the active control system on the noise barrier along the 20 m's high-way to reduce the noise of the "dark area". The active control system gained about 5 dB excess insertion loss in the factual situation. Berkhoff [8] used near-field error microphones to obtain the far-field error signals so as to control the far-field noise. This method improved the effectiveness of the active control system. The performance of the control algorithms are compared for far-field error signals, near-field error signals, and virtual far-field error signals. The simulations have shown that the performance of the virtual far-field error signals can gain the same results as the far-field error signals.

In anterior studies on the noise barriers with the active control system, the locations of the error microphones are on the top of the barriers, and the locations of the secondary sources are between the primary source and error microphones. This arrangement makes installation of the active system difficult in actual application. Through in the system introduced by Ohnishi et al. [7], the secondary sources are located beside the edge of the barrier, how to arrange the error microphones has not been mentioned. This will be investigated in this communication.

2. Theory

As shown in Fig. 1, when the noise barrier is interposed, the dash lines at $\theta = \pi - \theta_s$ and $\theta = \pi + \theta_s$ subdivided the field into three separated regions I–III. When the receiver is in region I, the total sound field is composed of directed sound by the primary source p_d, the reflected sound by the barrier p_r, and the diffracted sound by the edge of the barrier p_D. When the receiver is in region II, the total sound field is composed of directed sound by the primary source p_d, and the diffracted sound by the edge of the barrier p_D. When the receiver is in region III, namely "dark area", the diffracted sound only exists in the sound field. The formula of the total sound field p_p in each region is given, as follows:

$$\begin{aligned} &\text{Region I}: \quad p_p = p_d + p_r + p_D = \frac{A}{kR}e^{ikR} + \frac{A}{kR'}e^{ikR'} + p_D, \\ &\text{Region II}: \quad p_p = p_d + p_D = \frac{A}{kR}e^{ikR} + p_D, \\ &\text{Region III}: \quad p_p = p_D. \end{aligned} \tag{1}$$

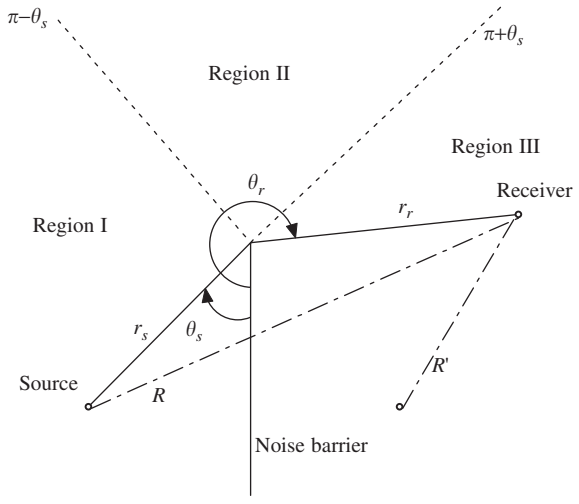

Fig. 1. Sketch map of the noise barrier.

The diffracted sound pressure in the "dark area" is calculated with MacDonald solution ($kR_1 \gg 1$) [4],

$$p_D = -\sqrt{\frac{2}{\pi k R_1}} A e^{-i\pi/4} \left\{ \mathrm{sgn}(\pi + \theta_s - \theta_r) \frac{e^{ikR}}{\sqrt{k(R_1 + R)}} F\left[\sqrt{k(R_1 - R)}\right] + \mathrm{sgn}(\pi - \theta_s - \theta_r) \frac{e^{ikR'}}{\sqrt{k(R_1 + R')}} F\left[\sqrt{k(R_1 - R')}\right] \right\}, \quad (2)$$

where k is the wavenumber of the sound, R and R' are, respectively, the distances from the receiver to the source and to the source mirror-image in the barrier. $R_1 = r_s + r_r$ is the shortest distance from the source to the receiver over the barrier top, $A = -iZ_0 q$, where q is the strength of the source, $Z_0 = \omega^2 \rho_0 / 4\pi c_0$, and $F(\mu) = \int_\mu^\infty e^{ix^2}\, dx$ is the Fresnel integral. The formula about calculating the diffracted sound pressure requires that the noise barrier is semi-infinite, and no reflected plane exists except the barrier. If there are other reflected planes in the positions of the source and the receiver, the influence of the reflection should be considered, such as the ground reflection may be considered with the image method.

When the ground reflections both of the source and the receiver are considered, when the receiver is in region III, the ground reflections on both sides of the barrier should be considered, and there are 4 pathways from primary source to the receiver over the barrier top (1) direct from the source to the receiver, (2) via the reflective ground on the source side, which is equivalent to the path from the source image to the receiver, (3) via the reflection ground on the receiving side, which is equivalent to the path from the source to the receiver image, and (4) via the reflective ground on both sides, which is equivalent to the path from the source image to the receiver image. The sound pressure in the receiver is given by $p_p = \sum_{i=1}^{4} p_{pi}$ [4].

The secondary sources are supposed as the monopoles, and there exists the direct sound and the ground reflected sound. So the sound pressure at location $\mathbf{r}$ by N_c secondary sources is [9]

$$p_c(\mathbf{r}) = \sum_{m=1}^{N} \left(\frac{i\omega\rho_0 q_m}{4\pi|\mathbf{r} - \mathbf{r}_m^c|} e^{-ik|\mathbf{r} - \mathbf{r}_m^c|} + \frac{i\omega\rho_0 q_m}{4\pi|\mathbf{r} - \mathbf{r}_{m'}^c|} e^{-ik|\mathbf{r} - \mathbf{r}_{m'}^c|} \right), \quad (3)$$

where q_m is the volume velocity of the mth secondary source, $\mathbf{r}_m^c$ the location of the mth secondary source, and ρ_0 the density of the air. The total sound pressure in location $\mathbf{r}$ is

$$p_t(\mathbf{r}) = p_p(\mathbf{r}) + p_c(\mathbf{r}) = \sum_{i=1}^{4} p_{pi}(\mathbf{r}) + \sum_{m=1}^{N} \left(\frac{i\omega\rho_0 q_m}{4\pi|\mathbf{r} - \mathbf{r}_m^c|} e^{-ik|\mathbf{r} - \mathbf{r}_m^c|} + \frac{i\omega\rho_0 q_m}{4\pi|\mathbf{r} - \mathbf{r}_{m'}^c|} e^{-ik|\mathbf{r} - \mathbf{r}_{m'}^c|} \right). \quad (4)$$

It is assumed that there are N_c secondary sources and N_e error sensors in this control system. The cost function to determine the optimal secondary source strength is to minimize the sum of the squared sound pressure:

$$J_p = \sum_{n=1}^{N_e} \left| p_t(\mathbf{r}_n^e) \right|^2 + \beta \mathbf{q}_s^H \mathbf{q}_s, \quad (5)$$

where $\mathbf{r}_n^e$ is the location of the nth error sensor and β the positive real number, which is used to determine the weighting for the control effort term. The optimal vector of the secondary source strength for the cost functions is given by [10]

$$\mathbf{q}_s = -(\mathbf{A} + \beta \mathbf{I})^{-1} \mathbf{b}, \quad (6)$$

where $\mathbf{A}=\mathbf{Z}_s^H\mathbf{Z}_s$, $\mathbf{b}=\mathbf{Z}_s^H\mathbf{p}_p$, $\mathbf{p}_p=\left[p_p(\mathbf{r}_1^e)\,p_p(\mathbf{r}_2^e)\,\ldots p_p(\mathbf{r}_{N'}^e)\right]^{\mathrm{T}}$, and

$$\mathbf{Z}_s=\begin{bmatrix} Z_{ce}(\mathbf{r}_1^e|\mathbf{r}_1^c) & Z_{ce}(\mathbf{r}_1^e|\mathbf{r}_2^c) & \ldots & Z_{ce}(\mathbf{r}_1^e|\mathbf{r}_M^c)\\ Z_{ce}(\mathbf{r}_2^e|\mathbf{r}_1^c) & & & \\ \vdots & & \ddots & \\ Z_{ce}(\mathbf{r}_N^e|\mathbf{r}_1^c) & & & Z_{ce}(\mathbf{r}_N^e|\mathbf{r}_M^c)\end{bmatrix},$$

$$Z_{ce}(\mathbf{r}_n^e|\mathbf{r}_m^c)=\frac{\mathrm{i}\omega\rho_0}{4\pi|\mathbf{r}_n^e-\mathbf{r}_m^c|}\mathrm{e}^{-\mathrm{i}k|\mathbf{r}_n^e-\mathbf{r}_m^c|}+\frac{\mathrm{i}\omega\rho_0}{4\pi|\mathbf{r}_n^e-\mathbf{r}_{m'}^c|}\mathrm{e}^{-\mathrm{i}k|\mathbf{r}_n^e-\mathbf{r}_{m'}^c|}.$$

After obtaining the optimal secondary source strength, it is substituted back to Eq. (4) to calculate the total sound pressure amplitude after control.

3. Numerical simulations and experiments

Experiments were carried out in the anechoic chamber of Nanjing University. Wood plates were used to cover the metal-grid floor to simulate real ground. The surface density of the plate is 14.1 kg/m^2 with the insertion loss of about 25.1 dB above 150 Hz. The dimension of the assumed semi-anechoic chamber is 11.2 m × 7.8 m × 5 m. The barrier was two wood plates thick, 1.22 m high, 4 m away from the wall inside the anechoic chamber, and the surface density of the barrier is 28.2 kg/m^2, the noise reduction is about 31.1 dB above 150 Hz. In this case, the sound transmission through the barrier can be ignored. The zero point of the coordinates is chosen at the middle of the crossing line between the barrier and the ground. The positive direction of x-, y-, and z-axis, respectively, goes to the door of the anechoic chamber, from the left to the right after entering the chamber, and up from the zero point. As shown in Fig. 2, the coordinates of the primary source are (−2, 0, 0.16) (the unit is meter), and the frequency of the noise was 160 Hz as the example. The observational points are chosen on the axes $z=0.1$ and 0.5 m. The coordinates of the observational points are point 1 (4, 0, 0.1), point 2 (5, 0, 0.1), point 3 (6, 0, 0.1), point 4 (4, 0, 0.5), point 5 (5, 0, 0.5), point 6 (6, 0, 0.5). Sixteen secondary sources are on the top of the barrier, and the space between them was 0.4 m. Sixteen error sensors are located near the corresponding secondary sources. The excess insertion losses just are the difference between the sound pressure levels, when the controller is on and off.

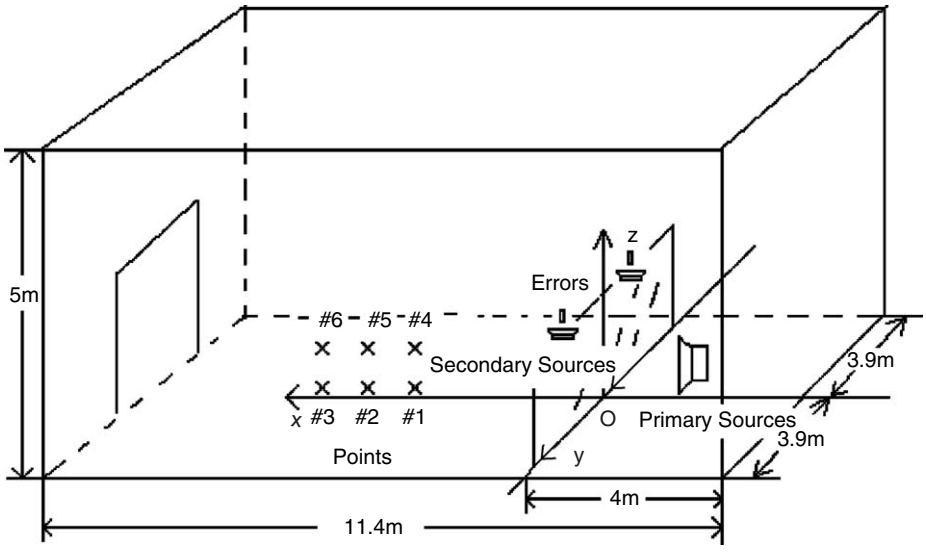

Fig. 2. Sketch map of the anechoic chamber and the experiment layout.

The measuring equipment is the PULSE Multianalyzer System. The type of the microphones for measurement is B&K 4190. The diameter of the loud speaker as the primary source is 32 cm and Power-amplifier is type 2706. A fiducial microphone of type B&K 4190 was used to ensure the constant of the radiated sound power from the primary source, 45 cm away from the center of the louder. The active control system consists of 16 speakers as the secondary sources, 16 microphones as error sensors, and a multichannel NDANC-I as the controller (see Fig. 3). The secondary sources were arranged on the sheet plate with 24 cm width on the top of the barrier. The positions of the error sensors were in the central axes of each secondary source. As shown Fig. 4, when the positions of the error sensors were changed, the secondary sources rotated along with the error sensors.

Three positions of the error sensors are discussed, respectively: (1) the error sensors are behind the secondary sources (between the primary source and the secondary sources); (2) the error sensors are above the secondary sources; (3) the error sensors are before the secondary sources (between the receiver and the secondary sources). The distance between the error sensors and the secondary sources is kept 0.08 m in all three configurations for comparing. The results for the far-field error sensors are also obtained for comparison, and the locations are on the line $x = 6$ m, $z = 0.2$ m, corresponding to the secondary sources.

The simulation results in Figs. 5 and 6 show that the excess insertion losses due to the active control system for all configurations are greater than 3 dB. When the error sensors are located in far field, close to the observational points, the excess insertion losses are the greatest. When the error sensors are arranged around the secondary sources, the effectiveness of the error sensors above the secondary sources is the best among those three arrangements, and the excess insertion losses in all observational points are over 6 dB. Fig. 7 shows the experiment results, where observational points 1–3 are at 0.1 m height and the observational points 4–6 are at 0.5 m height. For the three arrangements of the error sensors around the secondary sources, the effectiveness of the error sensors above the secondary sources is best, but the effectiveness of the error sensors before the secondary sources is close to it. This agree with the numerical simulations, so in the factual situation, the error sensors should be arranged above the secondary sources or before the secondary sources.

The simulation results in Fig. 8 show the variation of the excessive insertion loss with the distance between the error sensors and the secondary sources when the error sensors are above the secondary sources, which indicate that there exists an optimal distance for the greatest insertion loss in the "dark area". Although the optimal distances vary with different observational points, the distinctions between them are not large. It can be found in Fig. 8 that when the distance is 0.08 m, the excess ILs in all observational points are near to the

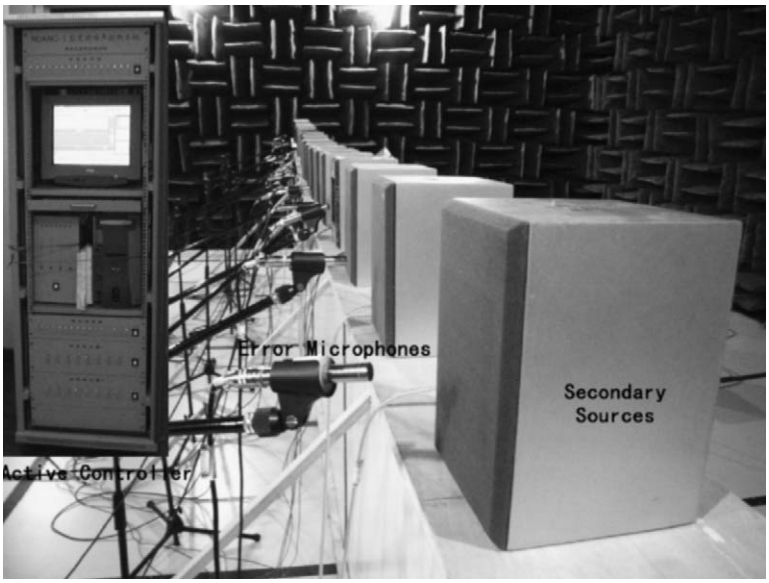

Fig. 3. The photo of the active soft edge noise barrier system with the controller.

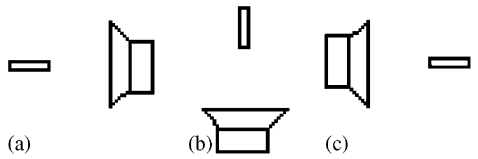

Fig. 4. Three arrangements of the error microphones and the secondary sources: (a) before, (b) above, and (c) behind the secondary sources.

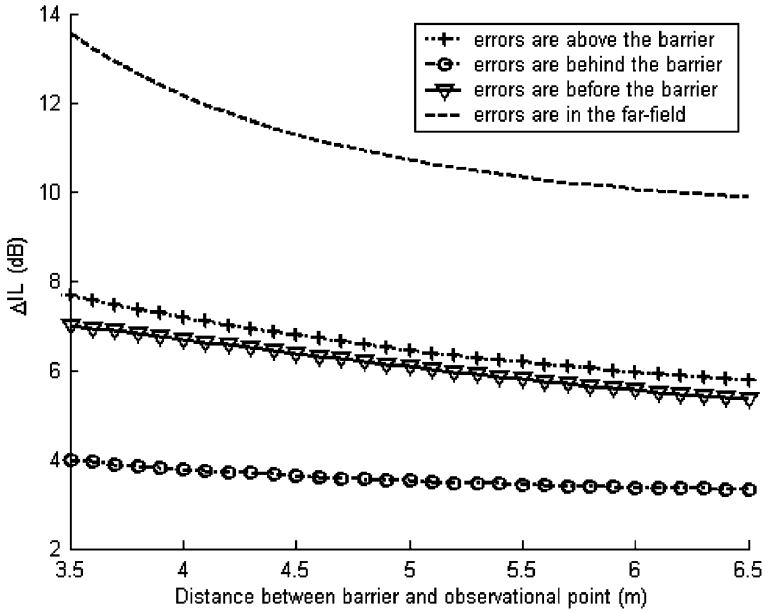

Fig. 5. Excess IL at the 0.1 m high observational points (simulation results).

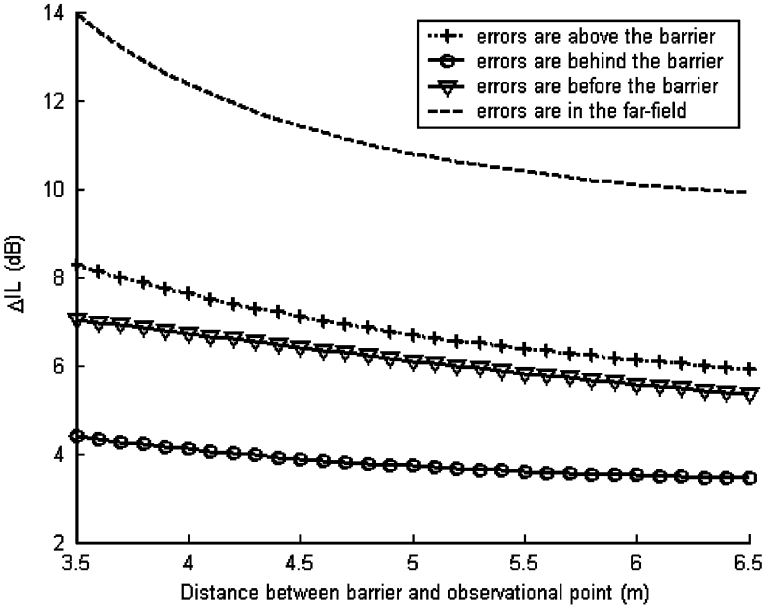

Fig. 6. Excess IL at the 0.5 m high observational points (simulation results).

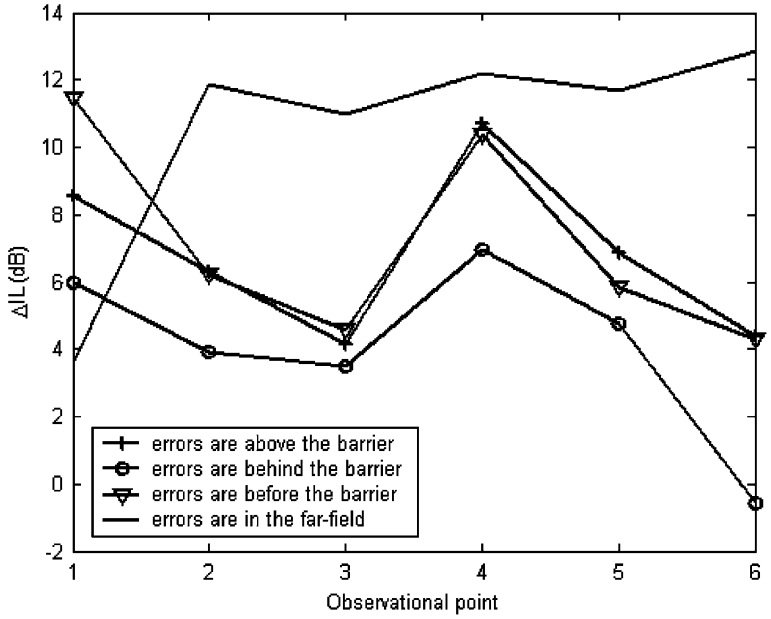

Fig. 7. Experimental excess IL of four arrangements in all observational points.

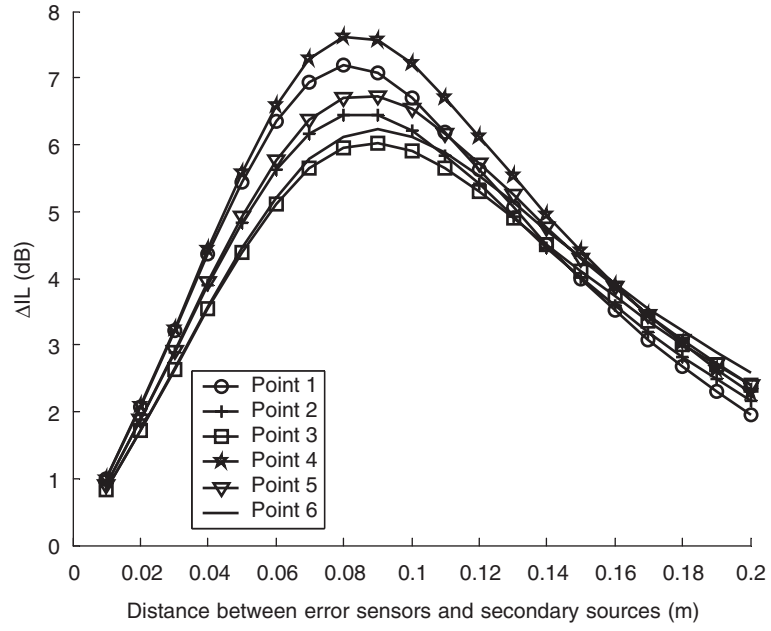

Fig. 8. The change curve of the excess IL in all observational points due to the distance between error sensors and control sources (simulation results).

greatest value, so when the distance is 0.08 m, the performance of the active control system is potent. Fig. 9 gives out the experiment results which agree with the numerical results.

Numerical simulations at other frequencies such as 125, 200, 250, 315 and 400 Hz have also been carried out, which confirm the above two conclusions. These results, however, are not included in the communication for brevity. From these results, it is found that there is an optimal distance between the error sensors and the secondary sources. The optimal distance depends on the noise frequency, the positions of the error sensors

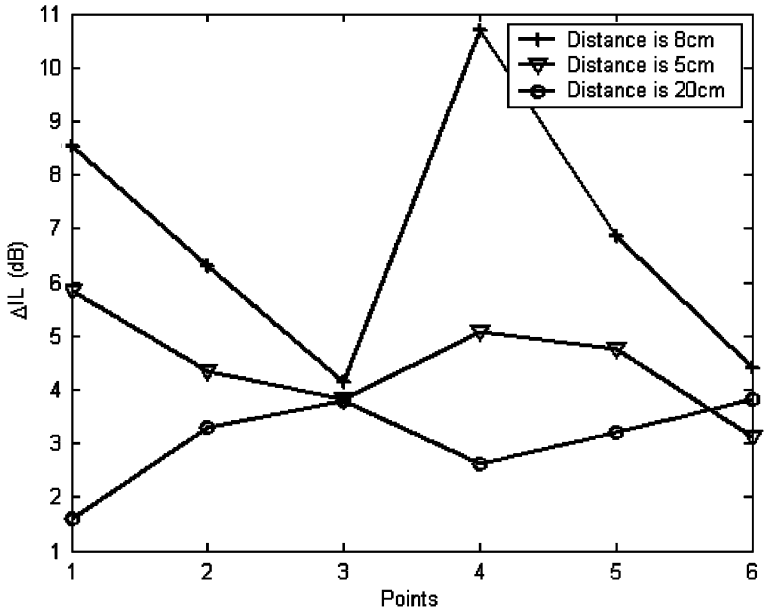

Fig. 9. Experimental excess IL in all observational points when the distance between error sensors and secondary sources is, respectively, 8, 5 and 20 cm.

arranged, and the selected observational points, but the influences due to the frequency and the selected observational points are not significant for frequencies below 500 Hz. Therefore, 8 cm is selected as the optimal distance to compromise most situations described in this communication when the error sensors are around the secondary sources.

The performance of the system will deteriorate for the broadband noise, which is the case for most active noise barrier applications. If a reference signal is possible, feedforward control can be used, the performance of the ANC system should be approach the results given in the paper depending on the coherence between the reference signal and error signals, and the positioning and the optimal distance between the secondary source and the error sensor might be still valid. If no reference signal is available, feedback control has to be used. Usually, feedback control system uses decentralized system, where each secondary loudspeaker only reduces the noise of the error sensor near this loudspeaker, and the minimum residual noise cannot be zero. Under these circumstances, the optimal position and distance might be different. This need to be further investigated in the future and it is quite possible that similar results can be obtained even for broadband control.

The effects of the active control system on the passive barrier can be considered as increasing the equivalent height of the noise barrier, and the corresponding height increased by the error sensors above the secondary sources is more than the other two, so the effect of the error sensors above the secondary sources is the best. On the other hand, some noise can also permeate through the space between the error sensors and the secondary sources to the ''dark area'' because the active system only minimizes the sound pressures around the error sensors. These two facts determines the optimize distance between the error sensors and the secondary sources when the sensors are above the secondary sources. The effect from the excess height is larger than that of the permeation when the distance is short. However, as the distance increases, the effect of the excess height due to increasing the distance becomes weaker, and the influence by the permeation becomes larger. When both of the effects are equal, the distance is the optimal for the maximum excess insertion loss.

4. Conclusions

This communication considered the optimization of the arrangement of error sensors for decreasing the noise in the ''dark area'' of an active soft edge noise barrier. Both numerical and the experimental results show that the best location for the error sensors in an active soft edge noise barrier are the places above the

secondary sources, and there also exists an optimal distance between the error sensors and the secondary sources for lager excess insertion loss under 500 Hz.

Acknowledgments

Project 10304008 supported by NSFC. The work was also sponsored by SRF for ROCS, SEM and SRFDP. The authors would like to extend sincere thanks to Mr. N.R. Li and Miss N. Han in Nanjing University, Prof. D. Fu and Mr. H. Min in Southeast University for their helpful assistance in the experiments, as well as to R.C. Wang who help me in English writing.

References

[1] K.M. Li, H.Y. Wong, A review of commonly used analytical and empirical formulae for predicting sound diffracted by a thin screen, *Applied Acoustics* 66 (2005) 45–76.
[2] A. Omoto, K. Fujiwara, A study of an actively controlled noise barrier, *Journal of the Acoustical Society of America* 94 (1993) 2173–2180.
[3] A. Omoto, K. Takashima, K. Fujiwara, Active suppression of sound diffracted by a barrier: an outdoor experiment, *Journal of the Acoustical Society of America* 102 (1997) 1671–1679.
[4] J. Guo, J. Pan, Increasing the insertion loss of noise barriers using an active-control system, *Journal of the Acoustical Society of America* 104 (1998) 3408–3416.
[5] J. Shao, J.-Z. Sha, Z.-L. Zhang, The method of the minimum sum of squared acoustic pressures in an actively controlled noise barrier, *Journal of Sound and Vibration* 204 (1997) 381–385.
[6] J. Yang, W.-S. Gan, On the actively controlled noise barrier, *Journal of Sound and Vibration* 240 (2001) 592–597.
[7] K. Ohnishi, T. Saito, S. Teranishi, Y. Namikawa, T. Mori, K. Kimura, K. Uesaka, Development of the product-type active soft edge noise barrier, *Proceedings of the18th International Congress on Acoustics*, Kyoto, Japan, 2004, pp. 1041–1044.
[8] A.P. Berkhoff, Control strategies for active noise barriers using near-field error sensing, *Journal of the Acoustical Society of America* 118 (2005) 1469–1479.
[9] X.J. Qiu, N.R. Li, G.Y. Chen, Feasibility study of developing practical virtual sound barrier system, *Proceedings of 12th International Congress on Sound and Vibration*, Lisbon, Portugal, 2005.
[10] P.A. Nelson, S.J. Elliott, *Active Control of Sound*, Academic Press, London, 1992.